Irrigation Science (2026) 44:1
https://doi.org/10.1007/s00271-025-01048-3

ORIGINAL PAPER

A comprehensive water balance approach for improved assimilation of evapotranspiration estimates derived from soil moisture

Diksha Chaudhary[1] · **Ickkshaanshu Sonkar**[1]

Received: 24 May 2025 / Accepted: 16 October 2025

Abstract
Advances in soil moisture monitoring techniques and sensor networks have made data assimilation a powerful tool for estimating evapotranspiration (ET). The commonly used simple water balance (SWB) model provides reliable ET estimates within the data assimilation framework. However, this approach often neglects the influence of ET on vertical fluxes. While this assumption is reasonable during the drying period in low-drainage soils, it may not hold in soils with high hydraulic conductivity. This study introduces a comprehensive water balance (CWB) model that explicitly accounts for ET-driven percolation. The model captures ET effects on vertical flux by comparing soil water depletion with and without ET, thereby highlighting the role of root water uptake (RWU) in percolation. The CWB model, combined with the ensemble Kalman filter, predicts daily ET by using soil moisture sensor data across different soil types. Within this framework, RWU rather than soil moisture serves as the observable for updating. The model's performance was evaluated against that of a SWB model under varying drainage conditions and with a reduced number of soil moisture sensors. The CWB model performed better than the conventional model in ET prediction, particularly in coarse-textured soils, reducing error by 45% and achieving higher accuracy (NSE = 0.918 vs. 0.727). ET prediction using eight sensors showed high accuracy (RV ≈ 1, NSE = 0.9, RMSE = 0.3 mmd^{-1}), while ET prediction using five sensors had slightly lower accuracy (RV > 0.75, NSE > 0.84, RMSE = 0.4 mmd^{-1}) but still provided reliable estimates under normal ET variations. Model testing with sensor errors showed that fine-textured soils exhibit lower sensitivity to uncertainty, enabling more reliable ET estimates. This finding highlights the necessity of incorporating vertical flux effects to avoid underestimation. Further improvement in prediction accuracy may be achieved by refining the bottom flux uncertainty within the framework. Even though this synthetic study shows the potential of RWU assimilation considering ET-affected percolation, future studies that focus on the use of real-field observations are necessary.

Keywords Evapotranspiration · Root water uptake · EnKF · Percolation · Data assimilation

Introduction

Evapotranspiration (ET) is an important hydrological process that is commonly predicted using physical models for water resource planning and management. ET comprises evaporation from the soil surface and transpiration in the form of root water uptake (RWU). Numerically, ET is computed mainly by solving the Richards equation, where RWU is represented as a sink term. The reduced RWU under abiotic stress is modeled using various empirical reduction functions with values ranging from 0 to 1 (Feddes 1974; Hoffman and Van Genuchten 1983). Physically, the RWU process can be simulated using a microscopic and a macroscopic approach. Macroscopic approach-based models are widely used because of their applicability in large-scale modeling (Baram et al. 2016; Oleson et al. 2008). Several studies have demonstrated the superior performance of matric flux potential-based RWU models, as they account for soil hydraulic potential (de Jong van Lier et al. 2013; de Melo et al. 2023; Iden et al. 2015). Additionally, the models implicitly incorporate the compensation mechanism of reduced RWU (de Jong van Lier et al. 2008).

With such physical models, the simulation of ET is a complex process influenced by both physical (Šimůnek

✉ Ickkshaanshu Sonkar
ickkshaanshu@iitrpr.ac.in

[1] Department of Civil Engineering, Indian Institute of Technology Ropar, Rupnagar, India

Published online: 20 November 2025

and Hopmans 2009; Wang et al. 2023; Yu et al. 2007) and biological processes (Javaux et al. 2013; Kalra et al. 2024; Vitali et al. 2021). However, ET estimation remains imprecise because of inherent uncertainties, including soil hydraulic and plant parameters (Baroni et al. 2010; Sonkar et al. 2019), surface boundary conditions (De Pue et al. 2019; Kumar et al. 2024; Rezaei et al. 2016) and representation of RWU as a sink term (dos Santos et al. 2017). These uncertainties have been handled well in research in the past decades by improving the existing physical models. The accuracy of such models has been improved through parameter estimation using inverse modeling (Angaleeswari et al. 2021; Cai et al. 2017; Kumar and Sonkar 2025; da Silva et al. 2020; Schelle et al. 2013) or by updating state variables and parameters through data assimilation techniques (Kandala et al. 2024; Li and Ren 2011; Orouskhani et al. 2023; Strebel et al. 2024). With advancements in low-cost sensors (Helmy et al. 2024; Levintal et al. 2022; Maya Moreshwar Meshram et al. 2024) and the development of soil moisture data networks (Dorigo et al. 2021), the scope of improving the ET estimation using data assimilation techniques has significantly increased in recent years.

Recently, the data assimilation approach has gained significant attention in estimating soil moisture, ET and leaf area index. Relevant studies utilise time series observations together with model predictions, accounting for their associated uncertainties to provide a more accurate representation of the system. For example, Li et al. (2021) and Li and Tartakovsky (2023) estimated hourly ET rates by using a soil moisture sensor array in 1D homogeneous and 2D heterogeneous soils, respectively. Through numerical experiments, these studies show that with the use of soil moisture observations, the ET predictions can be significantly improved with the ensemble Kalman filter (EnKF) technique. The methodology involves Bayesian updating of soil evaporation and RWU rate variables. These variables were corrected using the EnKF technique in conjunction with the simplified water balance (SWB) model of Breña Naranjo et al. (2011), which neglects ET's impact on vertical flow by assuming the same percolation rates with and without RWU. Such assumption holds well during the drying period in low-conductance soils, as used in these studies (Guderle and Hildebrandt 2015). However, vertical unsaturated flow is influenced by RWU, and this effect becomes noticeable when vertical flux is dominant, particularly in high-conductance soils, even during the drying period (Hupet et al. 2003; Sonkar et al. 2019). A similar phenomenon, where vertical flow remains comparable to RWU even days after a rainfall event, was observed by Schwärzel et al. (2009). Thus, considering the affected vertical flux while modeling the ET rate by using such water balance approaches is crucial. Moreover, the relevance of vertical flux increases as the modeling time step expands from hourly to daily.

The proposed study attempts to develop a comprehensive water balance (CWB) model that incorporates the influence of ET on vertical flow. Furthermore, the ET predictions of the CWB model are compared with those of the SWB model for high-conductance soil. The objective of this study is to develop and test a CWB model that estimates daily ET by using synthetic soil moisture data. Daily synthetic soil moisture data are generated from a numerical crop growth experiment. The ET rate simulation is based on a Bayesian update of the partial sink term, using soil moisture and simulated percolation information through the EnKF approach. The ET results from the CWB model are compared with those of the SWB model across different soil types to emphasise the importance of vertical flux (specifically percolation). Furthermore, the model's efficacy was tested under different soil types by reducing the number of sensors from eight to four to assess the impact of ET predictions on the number of soil moisture sensors. For this purpose, a 50-day crop growth numerical experiment was conducted to generate synthetic soil moisture data with known ET values.

Methodology

Root zone water dynamics

Root zone water flow is most commonly described using the one-dimensional Richards' equation (Clement et al. 1994). Equation (1), which describes unsaturated flow, was numerically solved along with the constitutive relationships (Eqs. 2–3). The solution was implemented using a mass-conservative, fully implicit finite difference FORTRAN code (Kumar et al. 2024)

$$\frac{\partial \theta}{\partial t} = \frac{\partial}{\partial z}\left[K(h)\left(\frac{\partial h}{\partial z} + 1\right)\right] - S(h, z, t) \tag{1}$$

where θ is the volumetric soil moisture [L^3L^{-3}], K is the unsaturated hydraulic conductivity [LT^{-1}], h refers to pressure head [L], t is the time [T], z denotes the vertical coordinate taken positive towards upward [L] and S is the sink term that describes water uptake by the root at given z and t [T^{-1}]. The above nonlinear equation was solved using the constitutive relations (non-hysteretic) θ-h and K-h proposed by van Genuchten (1980) and Mualem (1976), respectively. These relations describe the soil retention characteristics and are given as

$$\Theta = \begin{cases} \left[\frac{1}{1+|\alpha_v h|^{n_v}}\right]^{m_v} & for \ (h < 0) \\ 1 & for \ (h \geq 0) \end{cases} \tag{2}$$

and,

$$K = \begin{cases} K_s \Theta^{0.5}\left[1-\left(1-\Theta^{1/m_v}\right)^{m_v}\right]^2 & for\ (h<0) \\ K_s & for\ (h \geq 0) \end{cases} \quad (3)$$

where θ_s and θ_r are the volumetric saturated and residual soil moisture [L^3L^{-3}], respectively; α_v is the inverse of air-entry value [L^{-1}]; n_v denotes the index that depends on soil pore size [-]; m_v is the empirical parameter defined as 1-(1/n_v) [-], refers to the effective soil moisture defined as (θ-θ_r)/(θ_s –θ_r) [-]; and K_s is the saturated hydraulic conductivity [LT^{-1}].

The sink term (S) in Eq. (1) was calculated in terms of the transpiration rate, T [LT^{-1}], and the normalised distribution of RWU, $\lambda(z)$. The normalised distribution within root depth, z_r, was expressed as a function of root length density (RLD) and matric flux potential (M) (Eq. 4). Here, M was defined as $M(h) = \int_{h_w}^{h} K(h)\,dh$ (de Jong van Lier et al., 2008), where h_w is the pressure head at wilting point

$$\lambda(z,h) = \frac{RLD(z)\,M(h)}{\int_{L-Z_r}^{L} RLD(z)\,M(h)\,dz} \quad (4)$$

where $RLD(z) = RLD_{avg}(1+n)\left(1-\frac{L-z}{z_r}\right)^n$, RLD_{avg} is the average RLD [LL^{-3}], n is the nonlinear coefficient representing RWU distribution and L is the soil column length [L]. Thus, the sink term can be expressed as

$$S(h,z,t) = \lambda(z,h)\,T(t) \quad (5)$$

Furthermore, the distribution of RWU ensures that the $\int_0^{z_r} S(z)\,dz$ equals to T. The h values corresponding to θ=0.3 m^3m^{-3} were taken as the initial boundary condition. The top surface of the soil layer was treated as a Neumann-type boundary, representing evaporation/irrigation, given as

$$-K(h)\left(\frac{\partial h}{\partial z}+1\right) = q_{top}(t) \quad \text{at} \quad z = L,\ t > 0 \quad (6)$$

where q_{top} is the net flux due to irrigation and soil evaporation E_s at the top boundary, and L is the length of the soil column [L]. At the bottom, the water table was considered sufficiently deep to treat the bottom boundary as a free-drainage boundary. At the bottom boundary,

$$\frac{\partial h}{\partial z} = 0 \text{ at } z = 0,\ t \geq 0 \quad (7)$$

The RWU model was developed on the basis of Eqs. 1–7. With all soil hydraulic and RWU parameters known, the model can accurately simulate soil moisture for a given ET. For many realisations of the random inputs T and E_s, whose sum represents ET, the RWU model was run multiple times to generate realisations of θ. For accurate prediction of θ, reliable information on soil hydraulic properties and RWU parameters (root depth, average root length density and RWU distribution in this case) is essential. These parameters are often site-specific and subjected to uncertainties arising from soil heterogeneity and root development. Therefore, in a real-world experiment, prior information or calibration of these parameters is required. In this study, the proposed framework was restricted to homogenous soil, with the soil hydraulic and RWU parameters assumed to be static and either known or pre-estimated.

Sink term representation

Unlike the conventional approach of EnKF assimilation of soil moisture, this study considers the assimilation of partial RWU and E_s within the rooting depth (Li et al. 2021). The rooting depth [0, L] was divided into $N_{element}$ elements of length $\Delta z_{element}$, such that a sensor, if present, was placed at the centre of an element. For simplicity, uniform element length $s\,\Delta z_{element}$ were considered. According to Breña Naranjo et al. (2011), the water balance model for day n, which links soil moisture θ^n, infiltration rate I^n, percolation P_f^n and RWU^n, can be described as

$$ET^n = I^n - P_f^n - \sum_{i=1}^{N_{element}} \frac{\theta_i^n - \theta_i^{n-1}}{t_n - t_{n-1}}\,\Delta z_{element}, \quad n = 1, \ldots, N_{days} \quad (8)$$

where N_{days} is the number of days of simulation. For calculation, the CWB approach proposed that ET be estimated only during the dry period (Guderle and Hildebrandt 2015). Thus, ET can be estimated as

$$ET^n = -P_f^n - \sum_{i=1}^{N_{element}} \frac{\theta_i^n - \theta_i^{n-1}}{t_n - t_{n-1}}\,\Delta z_{element}, \quad n = 1, \ldots, N_{days} \quad (9)$$

Let $\theta^*(z,t^n)$ and $P_f^*(t^n)$ be the solutions to Eqs. 1–7 without considering ET losses, meaning $E_s \equiv 0$ and $T \equiv 0$ on the n^{th} day (Fig. 1). These solutions were obtained over a one-day interval $[t_{n-1}, t_n]$ using the initial condition when $n = 1$ or the water content calculated from the posterior mean of ET at time t_{n-1} when $n > 1$. From these simulations, θ_i^* for each i^{th} element and P_f^* were extracted on day n. In this case, the approximate root zone soil water depletion on the n^{th} day, using Eq. 9, can be written as

$$P_f^* = -\sum_{i=1}^{N_{element}} \frac{\theta_i^* - \theta_i^{n-1}}{t_n - t_{n-1}}\,\Delta z_{element} \quad (10a)$$

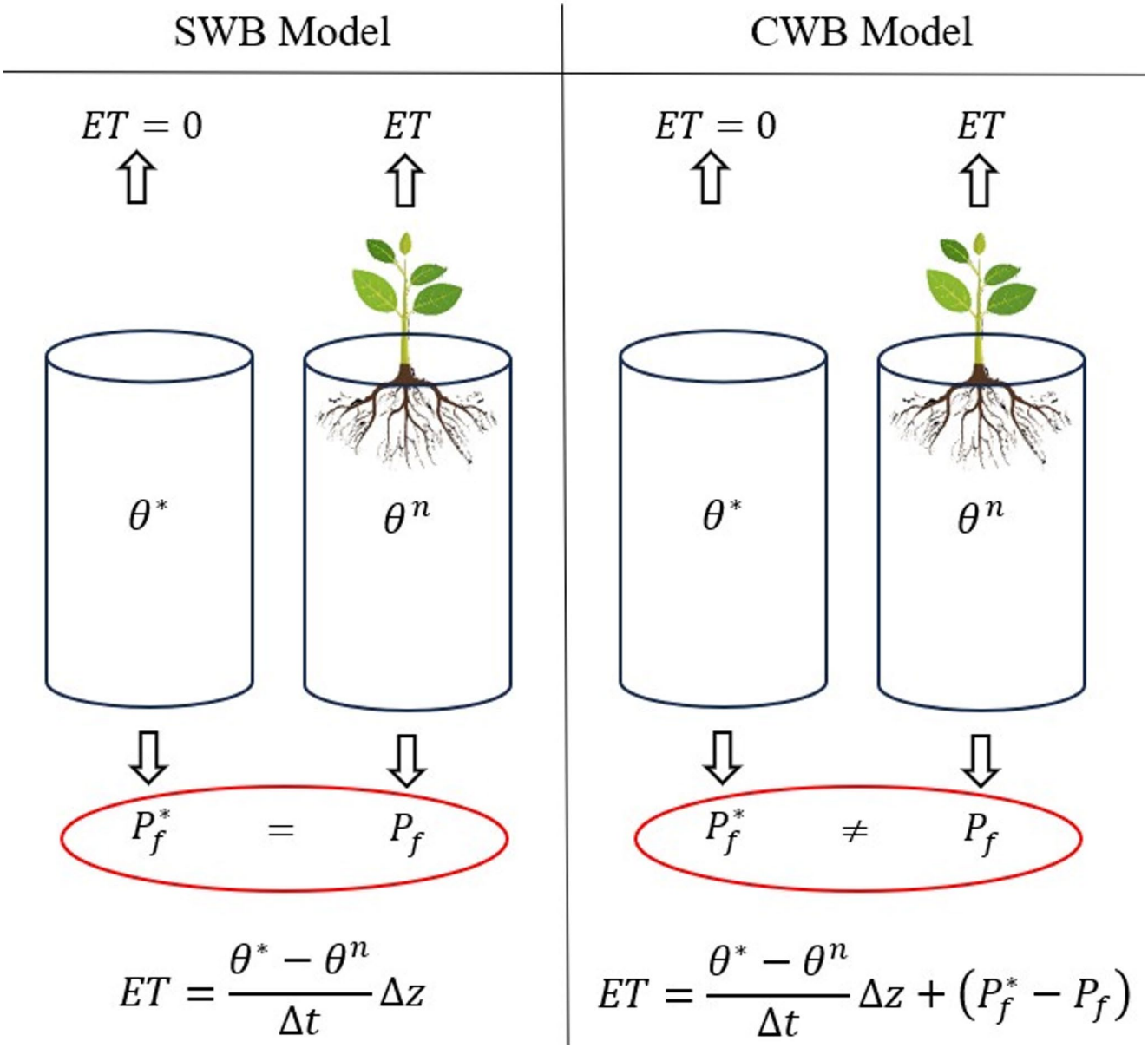

Fig. 1 ET computation in SWB and CWB approaches

Similarly, when ET is included, the full solution θ_i^n and P_f on the n^{th} day can be obtained, and root zone soil water depletion is expressed as

$$ET^n + P_f^n = -\sum_{i=1}^{N_{element}} \frac{\theta_i^n - \theta_i^{n-1}}{t_n - t_{n-1}} \Delta z_{element} \quad (10b)$$

Unlike the SWB approach (Li et al. 2021), the formulated equation considers the effect of ET on P_f (Fig. 1).

The first (i=1) element represents the top layer ET, $ET(z,t)\,\Delta z \equiv (E_s + T)\Delta z$, while in the remaining (i>1) elements, $ET(z,t) \equiv T$. Subtracting Eq. 10a from Eq. 10b and rearranging the terms give the following expression of ET^n:

$$ET^n = \sum_{i=0}^{N_{element}} \frac{\theta_i^* - \theta_i^n}{t_n - t_{n-1}} \Delta z_{element} + (P_f^* - P_f) \quad (11)$$

where $\frac{\theta_i^* - \theta_i^n}{t_n - t_{n-1}} \Delta z_{element}$ is the part of RWU $(S\Delta z)$ for each element, which is a function of soil moisture. This term, hereafter referred to as the partial sink term $\widehat{S}^n$, was updated using the Kalman filter.

Ensemble Kalman filter

The EnKF is a sequential data assimilation technique (Dong et al. 2016; Evensen 1994; Xiong et al. 2019) that employs an ensemble modeling approach, running multiple simulations simultaneously to estimate model uncertainty (Strebel et al. 2024). It uses the Monte Carlo method to approximate the error covariance matrix. This method considers the mean of the ensemble of model states evolving in the state space as the optimal estimate and represents the error covariance through the spread of the ensemble (Jiang et al. 2019). The process involves generating an ensemble of states, executing a model forecast and performing an analysis step by updating the states when observations become available.

The input parameters T and $E_s$between any two observation days t_{n-1} and t_n were considered independent Gaussian random variables. Their probability density functions (PDFs), $f_T\,(\epsilon_T)$ and $f_{E_s}\,(\epsilon_{E_s})$ had respective means μ_T and μ_{E_s} and standard deviations (SDs) σ_T and σ_{E_s}, which can be given as

$$f_a\,(\epsilon_a) = \frac{1}{\sqrt{2\pi\,\sigma_a^2}} e^{-\left[\frac{(\epsilon_a-\mu_a)}{2\sigma_a^2}\right]}, \qquad a = T, E_s \tag{12}$$

From the daily T and E_s values, the model simulated the partial sink term $\widehat{S}$ in Eq. (11). The predicted values of the $\widehat{S}(z,t)$ were arranged into a vector $\widehat{S}\,(t_n) = (\widehat{S}_1, \ldots, \widehat{S}_{N_{element}})^T$ of length $N_{element}$, considering $\widehat{S}(z,t)$ to be multivariate Gaussian (Li et al. 2021), with its PDF given as

$$f_s(\widehat{S};t_n) = \frac{1}{\sqrt{(2\pi)^{N_{element}}\left|\Sigma_{\widehat{S}}\right|}} e^{-\left[\frac{1}{2}(\widehat{S}-\mu_{\widehat{S}})^T \Sigma_{\widehat{S}}^{-1}(\widehat{S}-\mu_{\widehat{S}})\right]} \tag{13}$$

The $N_{element} \times 1$ vector of sample mean $\mu_{\widehat{S}}\,(t_n)$ and the $N_{element} \times N_{element}$ sample covariance matrix $\Sigma_{\widehat{S}}\,(t_n)$ were formulated using Monte Carlo realisations of $\widehat{S}\,(t_n)$ with a sample size of N_{sample}. On any measurement day t_n (n=1, …, N_{days}), the value of $\theta\,(z,t)$ at the sensor location N_{sms} was obtained from the RWU model, representing the synthetic soil moisture observation. White Gaussian noise v_i^n (i=1, …, N_{sms}) with zero mean and a specified observation error covariance $\Sigma_{\theta^n_{obs}}$ was generated to account for measurement noise. The soil moisture observation θ^n_{obs} was then obtained by adding v_i^n to the $\theta\,(z,t)$, given as

$$\theta^n_{obs} = \boldsymbol{\theta}\,(\boldsymbol{z},\boldsymbol{t}) + v_i^n \tag{14}$$

The $N_{sms} \times N_{element}$ observational matrix H^n_{obs} ensures that the numerical solution, computed with Δz and Δt, was available at the same locations and times as the observations θ^n_{obs}, which were collected with $\Delta\,z_{obs}$ and $\Delta\,t_{obs}$. If necessary, then interpolation was applied. The superscript n in H^n_{obs} indicates that this mapping was performed for time t_n. Instead of assimilating the soil–moisture data θ_{obs}, we assimilate the part of the actual sink term, ($\widehat{S}^n_{obs}$), defined for each element as

$$\widehat{S}^n_{obs} = \frac{(H^n_{obs}\theta^* - \theta_{obs})\Delta\,z_{obs}}{\Delta\,t_{obs}} \tag{15}$$

θ_{obs} follows a multivariate Gaussian; thus, its linear transformation $\widehat{S}_{obs}$ will also be a multivariate Gaussian, with a covariance matrix $\Sigma_{\widehat{S}_{obs}}\,(t_n)$, which can be described as

$$\Sigma_{\widehat{S}_{obs}}\,(t_n) = \frac{\Delta\,z^2}{\Delta\,t^2_{obs}}\Sigma_{\theta_{obs}}\,(t_n) \tag{16}$$

The posterior mean $\widehat{\mu}_{\widehat{S}}(t_n)$ and posterior covariance $\widehat{\Sigma}_{\widehat{S}}(t_n)$ of $\widehat{S}\,(t_n)$, obtained via the Kalman update, can be given as

$$\widehat{\mu}_{\widehat{S}} = \mu_{\widehat{S}} + K\left(\widehat{S}_{obs} - H^n_{obs}\mu_{\widehat{S}}\right) \tag{17}$$

where $N_{element} \times N_{sms}$ matrix K, which is called the Kalman gain, is given as

$$K = \Sigma_S H^{n^T}_{obs}(H^n_{obs}\Sigma_S H^{n^T}_{obs} + \Sigma_{S_{obs}})^{-1} \tag{18}$$

The implementation of the above methodology is described in Fig. 2.

Design of the numerical experiment

A 50-day crop growth scenario was considered with varying ET and irrigation fluxes throughout the growth period to generate synthetic soil moisture data (Fig. 3). An unsaturated flow model based on Eqs. (2)–(7) was developed for three scenarios: crop grown in (i) loam sand (LS), (ii) sandy loam (SL) and (iii) sandy clay loam (SCL). The soil hydraulic properties of these soils are detailed in Table 1. A 1.5 m homogeneous soil column was considered, with a spatial discretisation Δz=0.01 m, and a temporal discretisation Δt=15 min. The top boundary condition was defined as the atmospheric boundary, subjected to ET and irrigation fluxes, while the lower boundary condition was treated as free drainage. The atmospheric boundary conditions of 1-day resolution throughout the growth period are shown in Fig. 3a. During this period, a fully grown crop scenario was considered, characterised by a root depth of 1 m. The initial pressure head throughout the soil column was set to a value

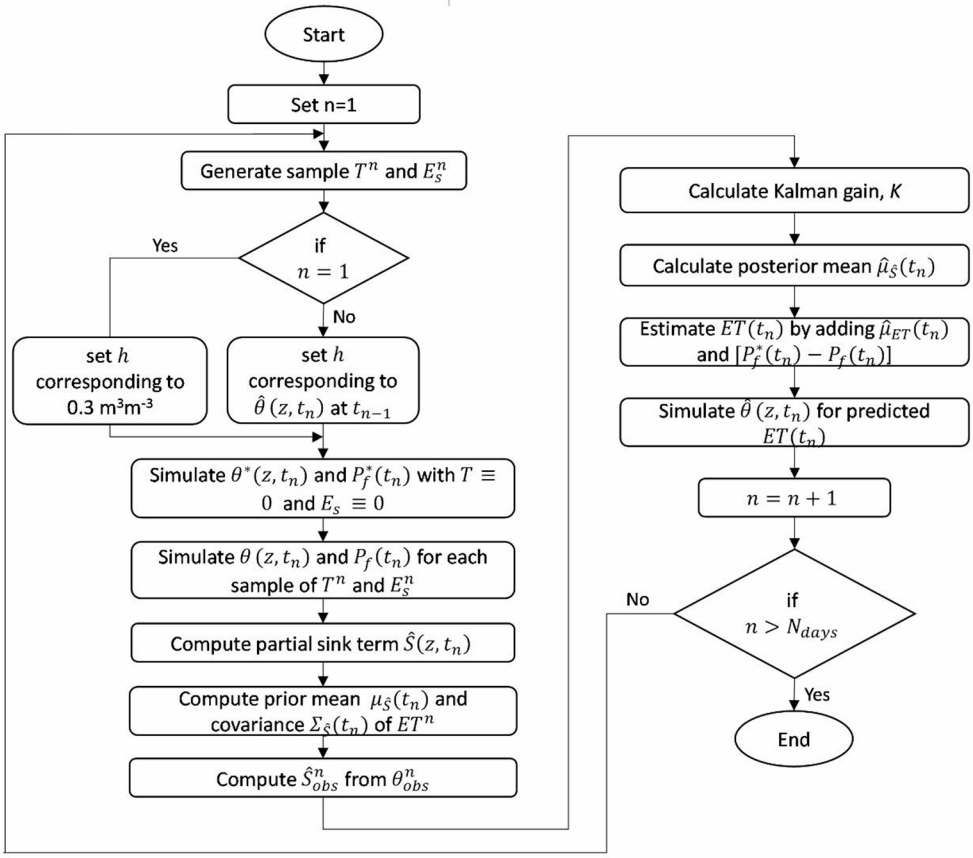

Fig. 2 Schematic framework of ET data assimilation

corresponding to soil moisture of 0.3 m^3m^{-3}. This initial condition provides a moist but unsaturated state across soils, ensuring active ET and percolation. With the use of these known parameters, initial condition and boundary conditions, a finite difference numerical code was run to simulate h and S for all the 151 nodes, along with E_s at the top node, at a temporal resolution of Δt.

From the simulated h at the end of the day, daily soil moisture (θ_{syn}) was calculated at each node. Similarly, cumulative E_s and T from S were calculated daily, with their sum representing the ET for that day. The obtained daily ET was treated as ET_{syn}. Additionally, the bottom flux at the lower boundary was cumulated daily to determine percolation (P_f). These simulations were performed for all three soil scenarios.

For ET predictions using the proposed algorithm, the root depth of 1 m was equally discretised into $N_{element} = 10$ segments of size 0.1 m. A soil moisture sensor was assumed to be placed at the centre of each element, recording soil moisture (θ_{obs}) that was obtained from the corresponding θ_{syn} at the respective depth and time. The sensors were placed in four setups: SMS8, SMS6, SMS5 and SMS4 (Table 2). The sensor setups show the reduction in the number of sensors from eight to four within the rooting depth. ET prediction was performed for three predefined crop growth scenarios. The simulated θ_{syn} and S for given irrigation and ET fluxes on a daily time scale for the SL soil case are shown in Fig. 3. During the growth period, six irrigation events were applied to cater to the ET demand. Each event increased soil moisture in the upper root zone, which then gradually decreased due to soil evaporation, RWU and vertical fluxes. The minimum soil moisture achieved was 0.124 m^3m^{-3}. The maximum RWU occurred within the top 30 cm root zone (Fig. 3c), which, along with soil evaporation, contributed to maximum soil moisture depletion (Fig. 3b).

To highlight the importance of percolation information, ET_{pred} was simulated using two models: (a) the SWB model, where the posterior ET for each day was calculated from Eq. (11) by assuming $P_f^* = P_f$, and (b) the CWB model, where the daily posterior ET was computed from Eq. (11), considering $P_f^* \neq P_f$. The simulation was performed for two scenarios: LS and SL. Each dry day was classified on the basis of relative soil water deficit (RSD) to evaluate prediction efficacy across different days within the irrigation interval. For each irrigation interval, RSD ranged from 0 to 1, where a value near 0 represented the least dryness (i.e. the day after irrigation) and a value close to 1 indicated maximum dryness (i.e. the day before irrigation). The RSD scatter plot allowed for an assessment of model performance

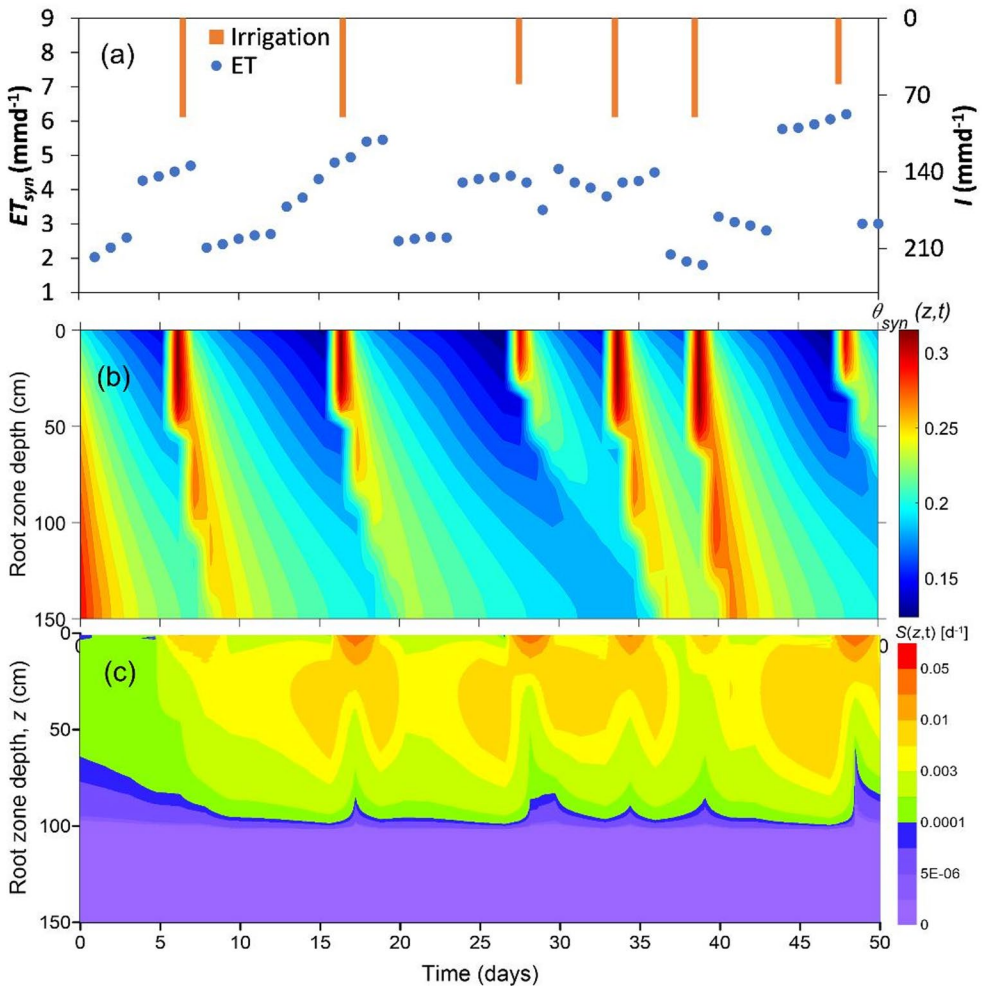

Fig. 3 Synthetic values of (**a**) ET and irrigation, (**b**) soil moisture and (**c**) RWU in SL soil

Table 1 Input mean soil hydraulic parameters taken from Carsel and Parrish (1988)

Soil type	θ_s (m^3m^{-3})	θ_r (m^3m^{-3})	α_v (cm^{-1})	n_v	K_s (md^{-1})
LS	0.41	0.057	12.4	2.28	3.50
SL	0.41	0.065	5.9	1.89	1.06
SCL	0.39	0.100	7.5	1.48	0.31

Table 2 Soil moisture sensor placement

Depth (m)	SMS8	SMS6	SMS5	SMS4
0.05	✓	✓	✓	✓
0.15	✓	✓	✓	✓
0.25	✓	✓	✓	-
0.35	✓	-	-	✓
0.45	✓	✓	✓	-
0.55	✓	-	-	✓
0.65	✓	✓	✓	-
0.75	-	-	-	-
0.85	✓	✓	-	-

under different soil moisture conditions. In all cases, ET predictions were made using the SMS8 setup.

Observation data

From the numerical experiment, soil moisture observations with measurement error were generated through three steps. Firstly, with the use of the known daily ET values, the RWU model with specified parameters was run to simulate soil moisture at each node and time step over 50 days. Secondly, daily soil moisture values at depths of 0.05, 0.15, 0.25, 0.35, 0.55, 0.65, 0.75 and 0.85 m were extracted from the simulation. These synthetic soil moisture values were treated as sensor observations. Finally, sensor error was added to the soil moisture data to represent measurement noise. For model performance evaluation, the standard deviation of the sensor error was initially set to 0.001 m^3m^{-3}. To further assess the predictive capability of the model under higher error levels, additional tests were conducted with observation errors of 0.01, 0.025 and 0.04 m^3m^{-3}. Comparative analyses were then performed for ET prediction using the SMS5 sensor setup under LS, SL and SCL scenarios.

Model performance evaluation

The efficacy of the model's ET predictions was evaluated using goodness of fit metrics, including the relative measure (RV) as defined in Li et al. (2021), the root-mean-square error (RMSE) and the Nash–Sutcliffe efficiency coefficient (NSE). The model's fitness was assessed through a comparison between predicted and synthetic daily ET values. These performance criteria were defined as

$$\mathrm{RV} = \frac{SD\prime}{SD^*} \tag{19}$$

$$\mathrm{RMSE} = \sqrt{\frac{\sum_{k=1}^{n}(ET' - ET^*)^2}{n}} \tag{20}$$

$$\mathrm{NSE} = 1 - \frac{\sum_{k}^{n}(ET' - ET^*)^2}{\sum_{k}^{n}(ET' - ET^*_m)^2} \tag{21}$$

where *SD'* and SD^* are the standard deviations of predicted and synthetic *ET* values, respectively; *ET'* and *ET** are the predicted and synthetic *ET*, respectively; ET^*_m is the mean of synthetic *ET* values and *n* is the number of data points of *ET*.

Results and discussion

The daily ET predictions were modeled using synthetically generated soil moisture (treated as θ_{obs}) corresponding to a known ET rate (ET_{syn}). For prediction, a crop growth numerical experiment was designed. The analysis includes ET predictions for LS, SL and SCL soils that were taken from Carsel and Parrish (1988). The ET predictions from the proposed CWB model and its comparison with the existing SWB model are performed in Sect. 3.1 and 3.2, respectively. Section 3.3 discusses the model's convergence rate. Section 3.4 examines the impact of the number of soil moisture sensors and observation error on ET prediction across the three soil types.

Evapotranspiration prediction

Figures 4 and 5 illustrate the daily ET estimates using eight and five sensors in the LS and SL scenarios, respectively. In both cases, the posterior ET rate (ET_{pred}) was simulated

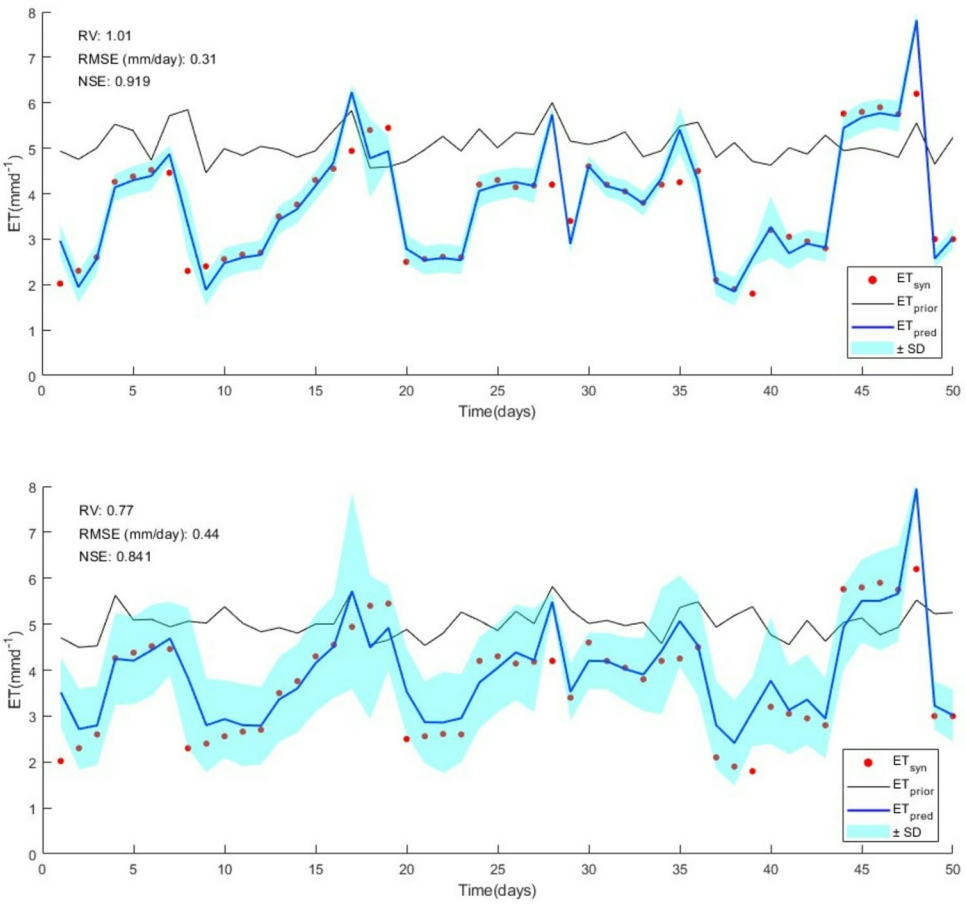

Fig. 4 Comparison of mean synthetic and predicted daily ET with prior mean ET information simulated with (a) SMS8 and (b) SMS5 soil moisture setups for LS. The predictions are accompanied by the confidence interval band as ± SD

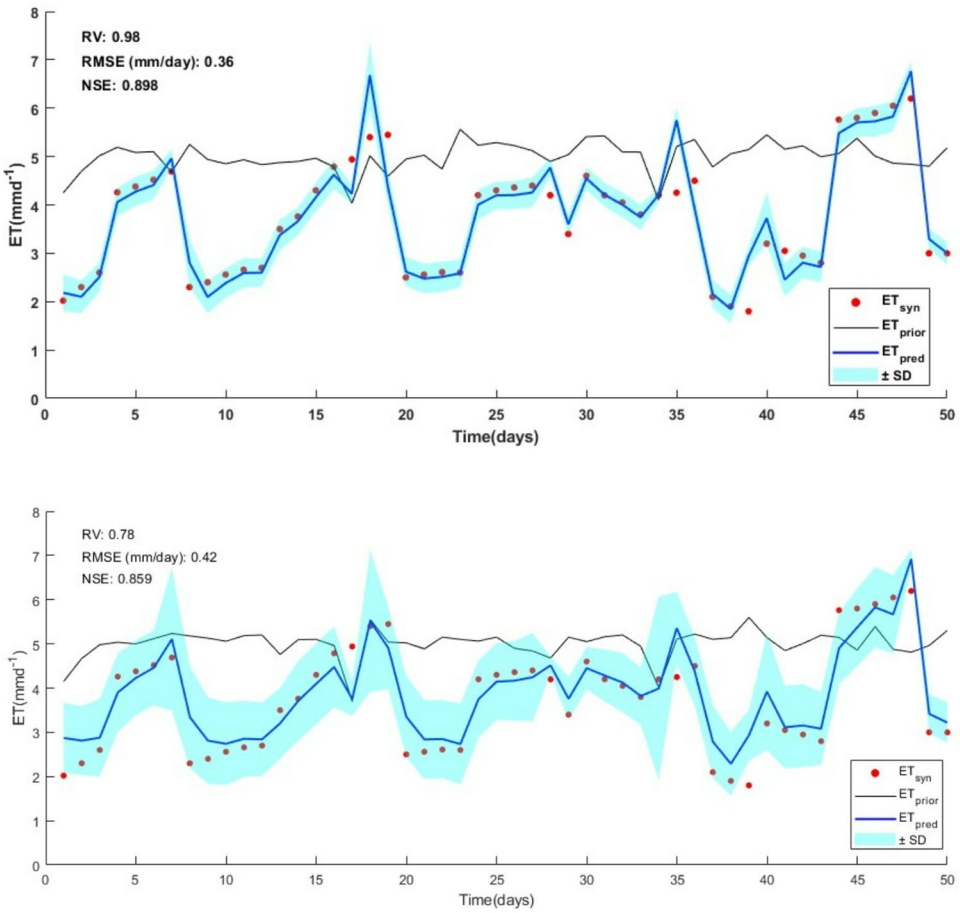

Fig. 5 Comparison of mean synthetic and predicted daily ET with prior mean ET information simulated with (a) SMS8 and (b) SMS5 setups for SL. The predictions are accompanied by the confidence interval band as ± SD

Table 3 Prior statistics of E_s and T

Variable	Value	Unit
Mean of E_s	2.0	mmd^{-1}
Standard deviation of E_s	1.5	mmd^{-1}
Mean of T	2.25	mmd^{-1}
Standard deviation of T	3.0	mmd^{-1}

using 150 ensemble realisations of the prior ET value. The ET value was the sum of T and E_s, which were obtained from their respective PDFs using the given mean and standard deviation values presented in Table 3. The approach of Li et al. (2021) was followed, which tested the model performance under high ET fluctuations, to evaluate the model's predictive capability under variable ET conditions. The model was assigned with an ET_{syn} daily series resembling a discontinuous function, where ET_{syn} ranged between 2 and 6.5 mmd^{-1} over a 50-day crop simulation period. Model fitness was assessed during the drying period (days without irrigation). ET predictions using eight sensors (SMS8) were highly accurate, with RV values close to 1 in both soil scenarios (Figs. 4a and 5a). Except on irrigation days, ET_{pred} showed strong agreement with synthetic values. This finding highlights the reliability of the proposed approach in predicting ET even under rapid soil drainage conditions. Deviations were primarily observed on irrigation days, which was expected because the given water balance approach could not estimate ET under these conditions (Guderle and Hildebrandt 2015). In both scenarios, the RMSE was approximately 0.3 mmd^{-1} and the NSE was 0.9, indicating the model's effectiveness in predicting ET using the SMS8 setup. The uncertainty band, defined by ± SD, covers the entire ET_{syn} dataset, except during irrigation events, where uncertainty in soil moisture dynamics led to deviations.

Compared with the case discussed above, ET prediction using five sensors (SMS5) was less accurate in both soil scenarios (Figs. 4b and 5b). However, the statistical indices indicated the good fitness of the model with an RV above 0.75 and an NSE greater than 0.84, suggesting the possibility of ET prediction with reduced soil moisture information. Moreover, the SMS5 setup was designed to place more sensors in the upper root zone, where maximum RWU occurs, as highlighted by Amiri et al. (2022). This strategic placement improved the prediction efficiency, resulting in a lower RMSE of 0.4 mmd^{-1}. However, the uncertainty band was broader than that of the ET prediction using the SMS8 setup. The increased uncertainty was primarily attributed to RWU estimation in unobserved locations, where RWU

values were corrected on the basis of correlations with observed depths. Reducing the number of sensors from eight to five led to a decrease in RV from 1 to 0.75, indicating lower variability in ET predictions. This finding suggests that while the model may not fully capture large ET fluctuations, it performs well under normal ET variations. This trend can be seen in Figs. 4 and 5, where the ET_{pred} line appears smoother than the predictions using the SMS8 setup. Overall, the comparison between SMS8 and SMS5 setups reveals that ET can be reasonably estimated with fewer sensors, provided that ET fluctuations are minimal and sensor placement is proportional to the RWU rate.

Here, the ET predictions from the model assume that the influence of interception is negligible, as ET is considered to result only from soil evaporation and transpiration (i.e. RWU). However, under actual field conditions, ET losses also include canopy evaporation, which mainly occurs during rainfall events and the following day (Baiamonte and Palermo 2022). The influence of canopy interception is more significant in regions with high rainfall and dense vegetation (Lai et al. 2023; Ngyuyen et al. 2021). Nevertheless, the CWB approach remains a simple and reliable method for estimating ET from soil moisture information, considering E_s and T as the main component.

ET prediction through SWB and CWB models

The comparisons of ET predictions for the LS and SL scenarios are shown in Figs. 6 and 7, respectively. For the LS scenario, the SWB model predictions were closer to the true value, particularly on drier days (RSD > 0.4). However, for most of the days with lower RSD, the model tended to underestimate ET values and showed a weak correlation (Fig. 6a). This underestimation occurred because the SWB model calculated ET as the difference in storage depth while ignoring changed vertical flow (Fig. 1). A similar observation was reported by Guderle and Hildebrandt (2015), where SWB approach-based models primarily focused on partial measurements of RWU. Overall, the SWB model exhibited above-average fitness with an RV of 1.15, indicating that the predictions were more extreme than the true values.

Compared with SWB simulation, the CWB model predictions showed a much stronger correlation with synthetic data, with an RV of 0.98 (Fig. 6b). Additionally, for lower RSD values, the CWB model predictions were significantly improved over the SWB model. However, ET predictions for wetter days (RSD < 0.4) still deviated from the true values, similar to the SWB model. This discrepancy was due to the limitation of using simulated P_f values for updating ET rather than observed data. These findings suggest that model accuracy could be further improved by incorporating percolation data with soil moisture measurements. In high-conductance soils such as LS, percolation becomes particularly relevant, as it provides additional information for modelling the RWU process (Sonkar et al. 2019). However, in field plot experiments where bottom flux data are unavailable, the CWB model is preferable over the SWB model, especially in high-conductance soils with considerable

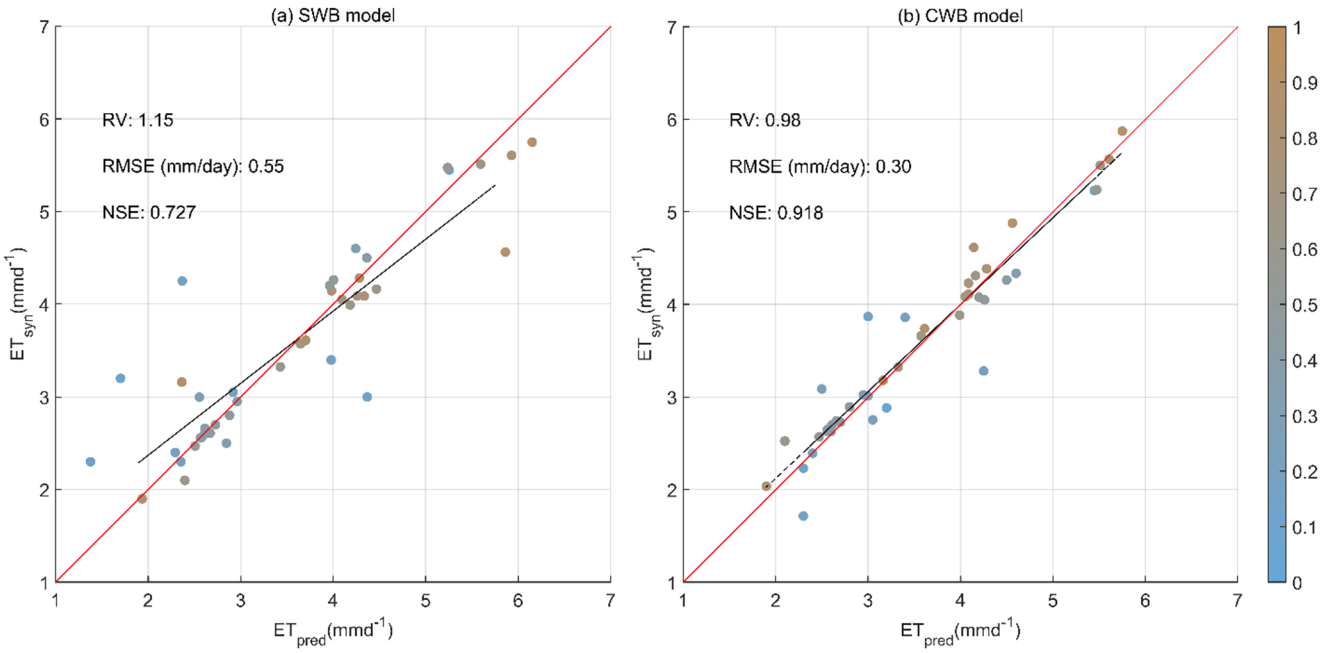

Fig. 6 Comparison of synthetic and predicted ET through (**a**) the SWB model and (**b**) the CWB model under the LS scenario. The colour gradient represents the relative soil water deficit of scattered points; blue (near 0) and brown (near 1) represent the lowest and highest soil water deficit of the day, respectively

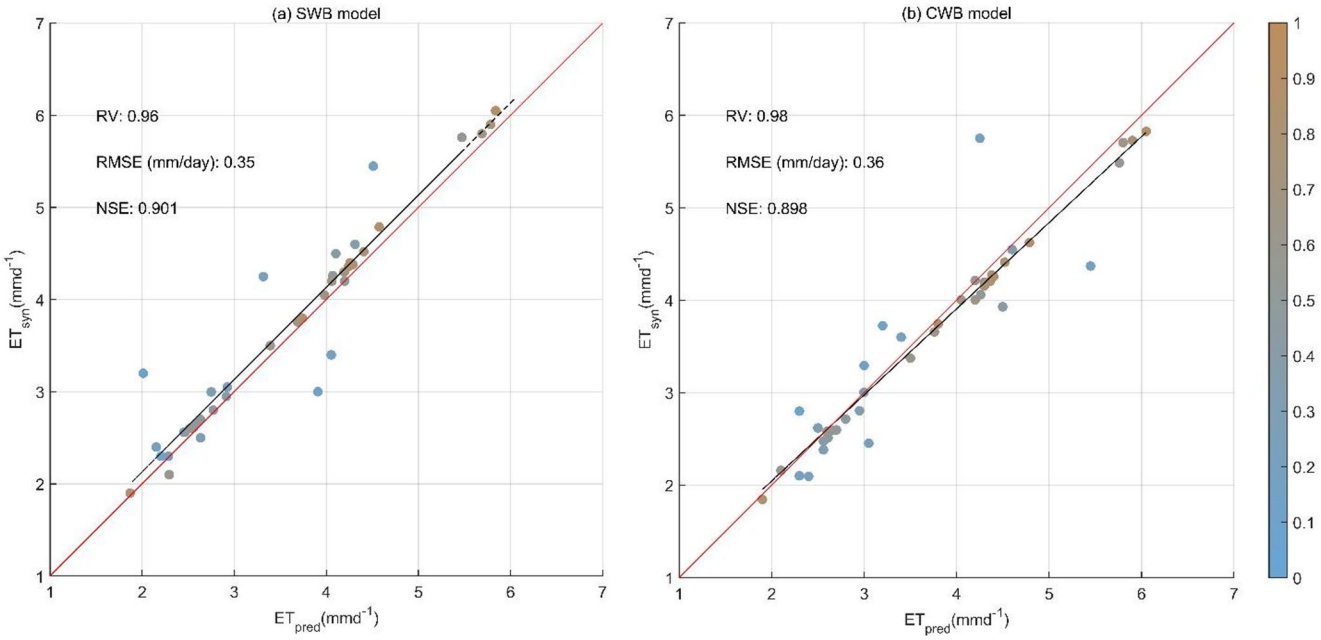

Fig. 7 Comparison of synthetic and predicted ET through (**a**) the SWB model and (**b**) the CWB model under the SL scenario. The colour gradient represents the relative soil water deficit of scattered points; blue (near to 0) and brown (near to 1) represent the lowest and highest soil water deficit of the day, respectively

precipitation/irrigation events. The NSE value of 0.918 for the CWB model indicates that it better captures *ET* variance compared with the SWB model (NSE = 0.727). Furthermore, the RMSE was significantly lower in the CWB, reducing the mean ET prediction error by 45% compared with the SWB model.

A similar comparative study was conducted for a relatively low-conductance soil scenario (SL), with comparison results presented in Fig. 7. Unlike in the LS scenario, both models performed well in SL soil. The SWB model showed a strong correlation with synthetic data, with RV = 0.96, RMSE = 0.35 mmd^{-1} and NSE = 0.901. Similar fitness statistics were observed for the CWB model. This finding indicates that the lower P_f and with high retention during wetter days did not significantly affect ET predictions. This finding aligns with the results of Li et al. (2021), who tested an SWB approach-based model at an hourly temporal scale with a single influx in low-conductance soil. However, the reliability of such an EnKF model in more practical scenarios defined by daily ET with multiple irrigation/precipitation events and varying drainage conditions still needs further investigation.

This study examines ET predictions across these scenarios. The results demonstrate that in coarse-textured soils, where substantial vertical flow occurs particularly early in the irrigation interval (lower RSD), neglecting bottom flux (as in the SWB model) can introduce significant errors in ET predictions using the EnKF technique. This study focuses on ET prediction using only soil moisture observation, which is why the proposed CWB model is a more suitable choice, especially in cases where vertical flow is expected to be more significant compared with RWU in physical models. The CWB model's ability to incorporate vertical flow makes it a more reliable ET predictor when using the RWU updating technique. This finding supports previous research on the influence of vertical flow on RWU rates (Hupet et al. 2003; Pollacco and Mohanty 2012; Sonkar et al. 2019).

Convergence rate

The model's performance in terms of convergence rate was tested using the previously defined RV, RMSE and NSE. The results are summarised in Table 4. The model was run for the LS, SL and SCL scenarios using the SMS5 sensor setup. Convergence was evaluated for different ensemble sizes N_{sample} of 50, 75, 100, 150 and 200. For most runs, the evaluation statistics remained nearly the same for N_{sample} = 100, 150 and 200. In all cases, once the ensemble size exceeded 150, the statistics remained unchanged, suggesting that N_{sample} = 150 was sufficient to achieve convergence. Therefore, for all the simulations in the study, an ensemble size of 150 was adopted for ET predictions.

Impact of the number of sensors and observation error

The study further investigated the model's prediction accuracy when the number of soil moisture sensors (N_{sms}) was

Table 4 Evaluation statistics for under different scenarios with varying N_{sample}

N_{sample}	LS soil			SL soil			SCL soil		
	RV (-)	RMSE (mmd^{-1})	NSE (-)	RV (-)	RMSE (mmd^{-1})	NSE (-)	RV (-)	RMSE (mmd^{-1})	NSE (-)
50	0.58	0.72	0.669	0.69	0.53	0.781	0.77	0.46	0.825
75	0.63	0.66	0.750	0.72	0.49	0.811	0.81	0.44	0.858
100	0.75	0.46	0.810	0.77	0.42	0.839	0.85	0.41	0.877
150	0.77	0.44	0.841	0.78	0.42	0.851	0.85	0.40	0.873
200	0.77	0.43	0.846	0.78	0.42	0.856	0.85	0.40	0.873

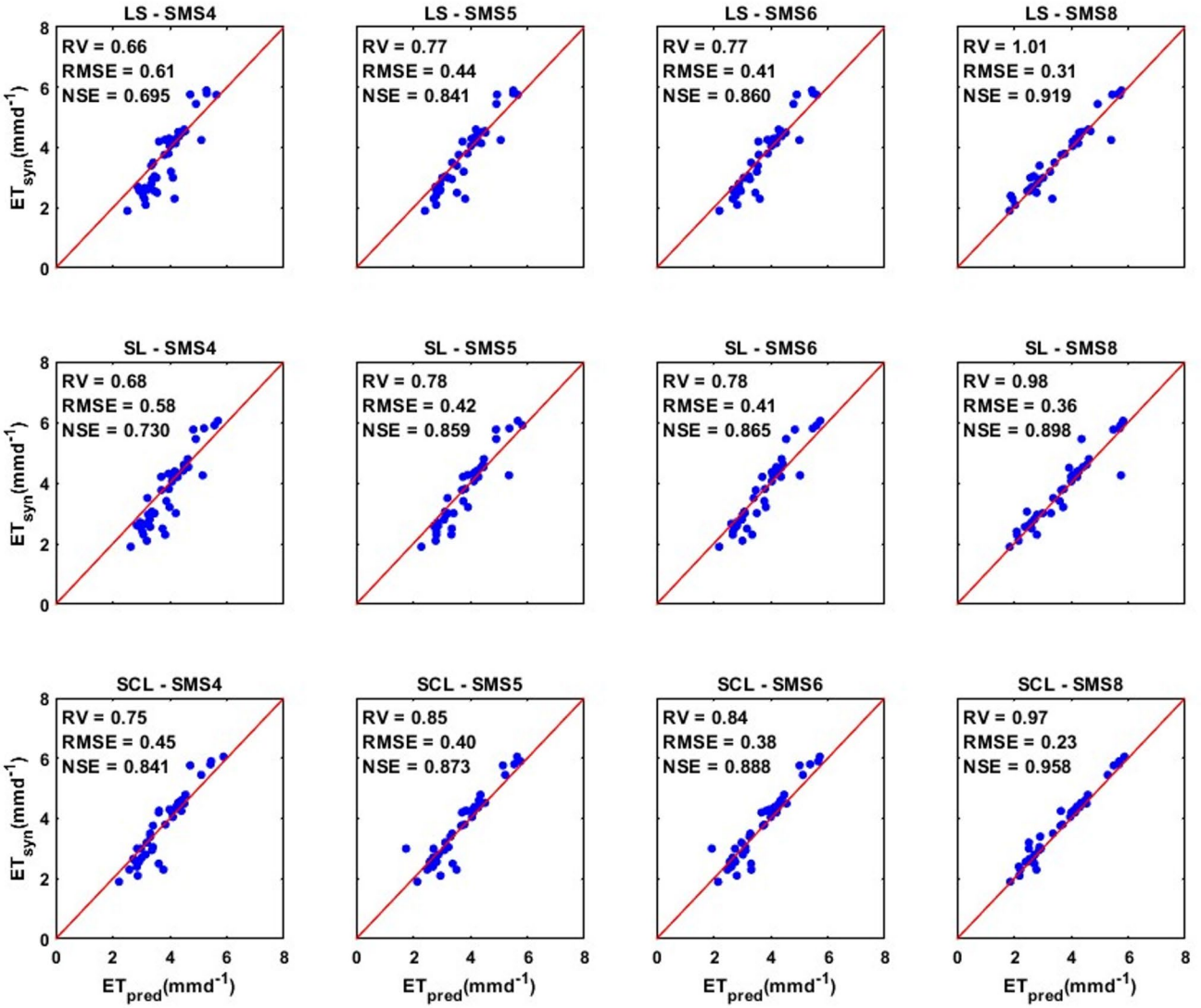

Fig. 8 Comparison of ET_{syn} with ET_{pred} estimated using different soil moisture sensor setup under (**a**) LS soil, (**b**) SL soil and (**c**) SCL scenarios

reduced from eight to four. ET predictions were based on the same numerical experiment setup defined earlier, which was run for LS, SL and SCL scenarios. Figure 8 demonstrates the impact of sensor count and placement on model performance.

The fitness evaluation showed that increasing the number of sensors improved prediction efficiency across all three scenarios. In the LS soil, the RMSE increased from 0.31 mmd^{-1} to 0.61 mmd^{-1} as the number of sensors decreased from 8 to 4. Additionally, the RMSE values were higher in the LS soil compared with those of corresponding setups in SL and SCL soils. The lowest RMSE (0.23 mmd^{-1}) was achieved in the SCL scenario using the SMS8 setup. The data clearly indicate that reducing the number of sensors

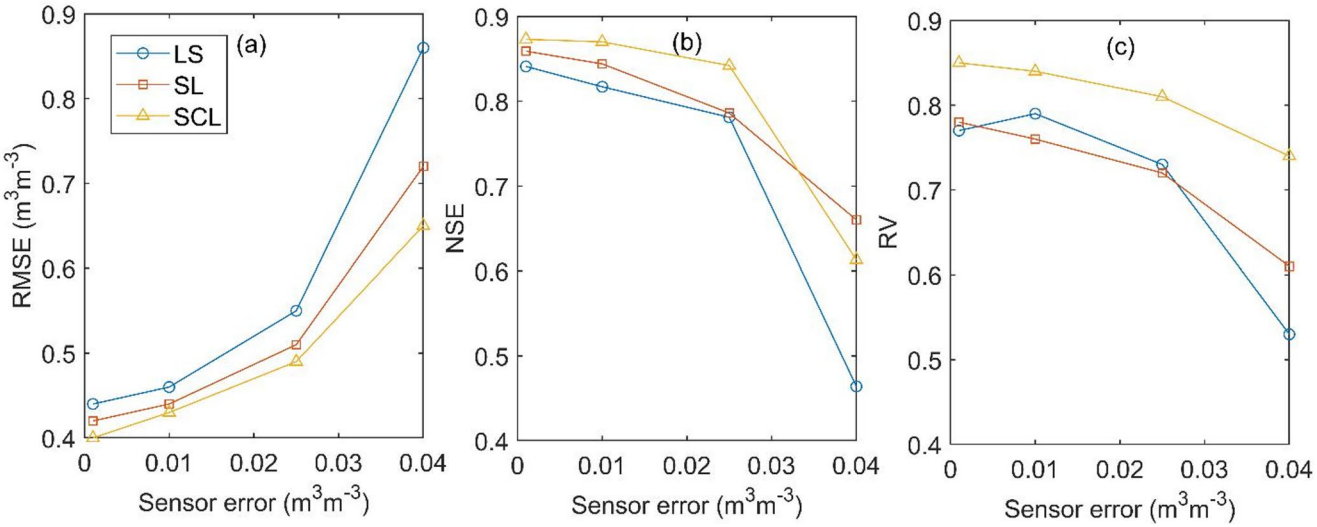

Fig. 9 Impact of the observation error on ET prediction using SMS5 setup

and increasing hydraulic conductance both contribute to greater uncertainty in ET prediction. This increased uncertainty arises because uncertainties in vertical flux were only partially addressed when considering simulated P_f for the RWU Bayesian update. However, incorporating P_f, which represents unsteady percolation, is important in high-conductance soils, as experimentally demonstrated by Bethune et al. (2008). This finding suggests that simulating vertical flux enhances RWU estimation through data assimilation, especially when soil moisture information is limited. The study contributes to advancements in ET extraction from enhanced soil moisture field data, which have become more accessible in recent decades due to improved monitoring techniques and sensor networks (Babaeian et al. 2019; Vereecken et al. 2008; Zhang et al. 2024).

Interestingly, even with four or five sensors, ET estimates remained reasonably accurate, with the NSE values consistently above 0.7 and often exceeding 0.8. This finding suggests that the model effectively correlates soil moisture at unobserved depths. However, predictive accuracy also depends on strategic sensor placement, ensuring sensors are positioned proportionally to RWU rate within rooting depth (Shen et al. 2018; Soulis et al. 2015). In LS soil, the RV value decreased from 0.9 to 0.69 when switching from the SMS8 to the SMS4 setup. A similar decreasing trend was observed in SL and SCL scenarios, where RV dropped from 0.89 to 0.73 and 0.95 to 0.84, respectively. This finding indicates that while ET predictions remained satisfactory with fewer sensors, higher fluctuation in ET requires the deployment of more sensors, especially in coarse-textured soils.

One of the important aspects of a data assimilation model is the quality of the observation data (Pauwels et al. 2007). In our study, soil moisture with realistic uncertainties was tested for ET simulations. Figure 9 shows the effect of different levels of sensor error (0.001–0.04 m^3m^{-3}) on ET estimation across LS, SL and SCL soils. The comparison of the predicted ET with the known ET highlights that prediction accuracy was highly sensitive to sensor error (Abolafia-Rosenzweig et al. 2019; Reichle et al. 2008), especially when the error exceeded 0.025 m^3m^{-3}. At a low error level (0.01 m^3m^{-3}), ET simulations performed well, with high NSE (>0.82), low RMSE (<0.46 mmd^{-1}) and RV values ranging between 0.76 and 0.84. Increasing the error to 0.025 m^3m^{-3} reduced model efficiency, with maximum RMSE reaching 0.55 m^3m^{-3} in LS. However, prediction accuracy was still much better than in the SMS4 setup (Fig. 8). The RV value ranged from 0.72 to 0.81 for errors up to 0.025 m^3m^{-3} in all scenarios, reflecting good agreement in ET variability. At the highest error level (0.04 m^3m^{-3}), prediction performance deteriorated substantially in all the scenarios, with RMSE ranging from 0.65 mmd^{-1} to 0.86 mmd^{-1}. Simulations using synthetic observations perturbed with smaller noise (0.001–0.025 m^3m^{-3}) consistently outperformed those with large observation errors (0.04 m^3m^{-3}). It is important to note, however, that these predictions were made under conditions of high ET variability. Under normal ET conditions, predictions are expected to perform better, even with a large sensor error. This finding is supported by the relatively small reduction in RV with increasing error, particularly in the SCL case.

The comparative analysis highlights the greater resilience of fine-textured soils (e.g. SCL) to sensor error. This is attributed to their higher storage capacity, which prevents the soil from reaching extremely dry states that may negatively affect EnKF performance (Han et al. 2012; Reichle et al. 2002). Overall, the results provide valuable guidance for the choice of a sensor setup and acceptable sensor error

across different soil drainage types, which must be carefully considered in soil moisture-based assimilation studies.

Conclusions

The study proposes a CWB approach for modeling ET rate using the EnKF data assimilation technique. The novel implementation of affected vertical flux due to ET in the CWB model aimed to enhance the prediction accuracy in LS, SL, and SCL. The methodology involves a Bayesian update of the partial sink term of Richards' equation rather than soil moisture. The daily updated sink term and affected bottom flux, influenced by ET, are used to compute ET for the next day. To achieve this, a 50-day numerical crop growth experiment that generates synthetic soil moisture observations for known ET was conducted. The CWB model performance was compared with that of the existing SWB model and assessed for its impact on prediction using limited soil moisture information. The analysis derived the following conclusions:

I. The CWB model performs better than the SWB model, particularly in coarse-textured soil (LS), where vertical flow remains significant compared with RWU even after irrigation. With lower RMSE and improved NSE, the CWB model demonstrates improved reliability under the tested conditions. Neglecting vertical flow can therefore lead to underestimation, especially in high-conductance soil.
II. ET prediction accuracy varies across the irrigation interval. The SWB model underestimates ET during the days following irrigation, whereas the CWB model maintains better correlation across both wetter and drier periods.
III. Reducing the number of sensors from eight to four results in smoother daily ET predictions with a broader uncertainty band, making it challenging for the CWB model to accurately capture large ET fluctuations. However, the model still provides reasonably accurate estimates with fewer sensors under normal ET variations.
IV. The study shows that even with fewer sensors, strategically placing them proportionally to RWU helps the CWB model maintain reliable ET predictions. Incorporating simulated percolation further improves prediction accuracy.
V. In low-conductance soils, both the SWB and CWB models perform similarly well, as vertical flow has less influence on ET. Under such conditions, either framework could potentially be applied, provided that sensors are strategically placed.
VI. The study highlights the importance of accounting for vertical flux in simulating ET, especially in coarse-textured soils. Where bottom flux information is unavailable, the CWB model may offer advantages for ET estimation, though field validation is required to confirm this potential.
VII. Even under a realistic degree of error in the soil moisture sensor (≈ 0.025 m^3m^{-3}), the model results benefit from the framework. However, prediction accuracy decreases significantly when the error increases to 0.04 $m^{-3}m^{-3}$.
VIII. Fine-textured soils such as SCL exhibit greater resilience to observation noise, as their higher storage capacity reduces the likelihood of reaching extremely dry states that strongly degrade assimilation performance.

To further enhance ET estimation, future research will incorporate uncertainties that may arise from soil heterogeneity, RWU parameters and lateral flow. Extending the model to 2D/3D flow domains and validating it against experimental or field data will strengthen its applicability.

Acknowledgements The authors are thankful to the Indian Institute of Technology Ropar, India for providing research support to carry out the research work.

Author contributions D.C. and I.S. contributed to the study conception, methodology and investigation. Material preparation, data collection, and analysis were performed by D.C. The first draft of the manuscript was written by D.C. and I.S., and both authors commented on previous versions of the manuscript. Both authors read and approved the final manuscript.

Funding No funding was received to assist with the preparation of this manuscript.

Data availability The present model is available through Chaudhary & Sonkar, (2025). Analysis and figures presented in this manuscript were made using MATLAB R2023a software available at www.mathworks.com (MATLAB, 2023).

Declarations

Conflict of interest The authors have no relevant financial or non-financial interests to disclose.

References

Abolafia-Rosenzweig R, Livneh B, Small EE, Kumar SV (2019) J Adv Model Earth Syst 11(11):3670–3690. https://doi.org/10.1029/2019MS001797. Soil Moisture Data Assimilation to Estimate Irrigation Water Use

Amiri Z, Gheysari M, Mosaddeghi MR, Amiri S, Tabatabaei MS (2022) An attempt to find a suitable place for soil moisture sensor

in a drip irrigation system. Inform Process Agric 9(2):254–265. https://doi.org/10.1016/j.inpa.2021.04.010

Angaleeswari M, Ravikumar V, Kannan SV (2021) Evapotranspiration estimation by inverse soil water flow modelling. Irrig Sci 39(5):633–649. https://doi.org/10.1007/s00271-021-00734-2

Babaeian E, Sadeghi M, Jones SB, Montzka C, Vereecken H, Tuller M (2019) Ground, proximal, and satellite remote sensing of soil moisture. Rev Geophys 57(2):530–616. https://doi.org/10.1029/2018RG000618

Baiamonte G, Palermo S (2022) Measuring and modelling evaporation losses from wet branches of lemon trees. Hydrology 9(7):118. https://doi.org/10.3390/hydrology9070118

Baram S, Couvreur V, Harter T, Read M, Brown PH, Kandelous M, Smart DR, Hopmans JW, Modeling HYDRUS (2016) Vadose Zone J, 15(11), 1–13. https://doi.org/10.2136/vzj2016.07.0061

Baroni G, Facchi A, Gandolfi C, Ortuani B, Horeschi D, van Dam JC (2010) Uncertainty in the determination of soil hydraulic parameters and its influence on the performance of two hydrological models of different complexity. Hydrol Earth Syst Sci 14(2):251–270. https://doi.org/10.5194/hess-14-251-2010

Bethune MG, Selle B, Wang QJ (2008) Understanding and predicting deep percolation under surface irrigation. Water Resour Res 44(12). https://doi.org/10.1029/2007WR006380

Breña Naranjo JA, Weiler M, Stahl K (2011) Sensitivity of a data-driven soil water balance model to estimate summer evapotranspiration along a forest chronosequence. Hydrol Earth Syst Sci 15(11):3461–3473. https://doi.org/10.5194/hess-15-3461-2011

Cai G, Vanderborght J, Couvreur V, Mboh CM, Vereecken H (2017) Parameterization of root water uptake models considering dynamic root distributions and water uptake compensation. Vadose Zone J 17(1):1–21. https://doi.org/10.2136/vzj2016.12.0125

Carsel RF, Parrish RS (1988) Developing joint probability distributions of soil water retention characteristics. Water Resour Res 24(5):755–769. https://doi.org/10.1029/WR024i005p00755

Chaudhary D, Sonkar I (2025) A comprehensive water balance approach for improved assimilation of evapotranspiration estimates derived from soil moisture [Model]. Zenodo. https://doi.org/10.5281/zenodo.14986057

Clement TP, Wise WR, Molz FJ (1994) A physically based, two-dimensional, finite-difference algorithm for modeling variably saturated flow. J Hydrol 161(1–4):71–90. https://doi.org/10.1016/0022-1694(94)90121-X

da Silva AJP, Pinheiro EAR, de Jong Q (2020) Determination of soil hydraulic properties and its implications for mechanistic simulations and irrigation management. Irrig Sci 38(3):223–234. https://doi.org/10.1007/s00271-020-00664-5

de Jong Q, van Dam JC, Metselaar K, de Jong R, Duijnisveld WHM (2008) Macroscopic root water uptake distribution using a matric flux potential approach. Vadose Zone J 7(3):1065–1078. https://doi.org/10.2136/vzj2007.0083

de Jong Q, van Dam JC, Durigon A, dos Santos MA, Metselaar K (2013) Modeling water potentials and flows in the Soil–Plant system comparing hydraulic resistances and transpiration reduction functions. Vadose Zone J 12(3):1–20. https://doi.org/10.2136/vzj2013.02.0039

de Melo MLA, de Jong Q, Cichota R, Pollacco JAP, Fernández-Gálvez J, Pahlow M (2023) Sensitivity analysis of land and water productivities predicted with an empirical and a process-based root water uptake function. J Hydrol 626:130241. https://doi.org/10.1016/j.jhydrol.2023.130241

De Pue J, Rezaei M, Van Meirvenne M, Cornelis WM (2019) The relevance of measuring saturated hydraulic conductivity: sensitivity analysis and functional evaluation. J Hydrol 576:628–638. https://doi.org/10.1016/j.jhydrol.2019.06.079

Dong Q, Zhan C, Wang H, Wang F, Zhu M (2016) A review on evapotranspiration data assimilation based on hydrological models. J Geog Sci 26(2):230–242. https://doi.org/10.1007/s11442-016-1265-4

Dorigo W, Himmelbauer I, Aberer D, Schremmer L, Petrakovic I, Zappa L, Preimesberger W, Xaver A, Annor F, Ardö J, Baldocchi D, Bitelli M, Blöschl G, Bogena H, Brocca L, Calvet J-C, Camarero JJ, Capello G, Choi M, Sabia R (2021) The international soil moisture network: serving Earth system science for over a decade. Hydrol Earth Syst Sci 25(11):5749–5804. https://doi.org/10.5194/hess-25-5749-2021

dos Santos MA, de Jong Q, van Dam JC, Bezerra F, A. H (2017) Benchmarking test of empirical root water uptake models. Hydrol Earth Syst Sci 21(1):473–493. https://doi.org/10.5194/hess-21-473-2017

Evensen G (1994) Sequential data assimilation with a nonlinear quasi-geostrophic model using Monte Carlo methods to forecast error statistics. J Phys Res 99(C5). https://doi.org/10.1029/94jc00572

Feddes RA (1974) Field test of a modified numerical model for water uptake by root systems. Water Resour Res 10(6):1199–1206. http://onlinelibrary.wiley.com/doi/ https://doi.org/10.1029/WR010i006p01199/full

Guderle M, Hildebrandt A (2015) Using measured soil water contents to estimate evapotranspiration and root water uptake profiles— a comparative study. Hydrol Earth Syst Sci 19(1):409–425. https://doi.org/10.5194/hess-19-409-2015

Han E, Merwade V, Heathman GC (2012) Implementation of surface soil moisture data assimilation with watershed scale distributed hydrological model. J Hydrol 416–417:98–117. https://doi.org/10.1016/j.jhydrol.2011.11.039

Helmy HS, Abuarab ME, Abdeldaym EA, Abdelaziz SM, Abdelbaset MM, Dewedar OM, Molina-Martinez JM, El-Shafie AF, Mokhtar A (2024) Field-grown lettuce production optimized through precision irrigation water management using soil moisture-based capacitance sensors and biodegradable soil mulching. Irrig Sci. https://doi.org/10.1007/s00271-024-00969-9

Hoffman G, Van Genuchten J (1983) M Th. Soil properties and efficient water use: water management for salinity control 73–85 https://doi.org/10.2134/1983.limitationstoefficientwateruse.c5

Hupet F, Lambot S, Feddes RA, van Dam JC, Vanclooster M (2003) Estimation of root water uptake parameters by inverse modeling with soil water content data. Water Resour Res 39(11):1–16. https://doi.org/10.1029/2003WR002046

Iden SC, Peters A, Durner W (2015) Improving prediction of hydraulic conductivity by constraining capillary bundle models to a maximum pore size. Adv Water Resour 85:86–92. https://doi.org/10.1016/j.advwatres.2015.09.005

Javaux M, Couvreur V, Vanderborght J, Vereecken H (2013) Root water uptake: from three-dimensional biophysical processes to macroscopic modeling approaches. Vadose Zone J 12(4):0. https://doi.org/10.2136/vzj2013.02.0042

Jiang Z, Huang Q, Li G, Li G (2019) Parameters estimation and prediction of water movement and solute transport in layered, variably saturated soils using the ensemble Kalman filter. Water (Switzerland) 11(7). https://doi.org/10.3390/w11071520

Kalra A, Goel S, Elias AA (2024) Understanding role of roots in plant response to drought: way forward to climate-resilient crops. Plant Genome 17(1). https://doi.org/10.1002/tpg2.20395

Kandala R, Franssen HH, Chaudhuri A, Sekhar M (2024) The value of soil temperature data versus soil moisture data for state, parameter, and flux Estimation in unsaturated flow model. Vadose Zone J 23(1). https://doi.org/10.1002/vzj2.20298

Kumar A, Sonkar I (2025) Estimability analysis and optimization of soil hydraulic and abiotic stress parameters from root zone saltwater dynamics in soil column lysimeter. Plant Soil. https://doi.org/10.1007/s11104-024-07167-8

Kumar A, Sonkar I, Sarmah R (2024) Modeling root zone water and salt transport using matric flux potential based root water uptake distribution. J Hydrol 630:130712. https://doi.org/10.1016/j.jhydrol.2024.130712

Lai Y, Tian J, Kang W, Guo S, Zhou Y, He C (2023) Estimating evapotranspiration from soil moisture using the improved soil water balance method in cold mountainous areas. J Hydrology X 20:100154. https://doi.org/10.1016/j.hydroa.2023.100154

Levintal E, Ganot Y, Taylor G, Freer-Smith P, Suvocarev K, Dahlke HE (2022) An underground, wireless, open-source, low-cost system for monitoring oxygen, temperature, and soil moisture. SOIL 8(1):85–97. https://doi.org/10.5194/soil-8-85-2022

Li C, Ren L (2011) Estimation of unsaturated soil hydraulic parameters using the ensemble Kalman filter. Vadose Zone J 10(4):1205–1227. https://doi.org/10.2136/vzj2010.0159

Li W, Tartakovsky DM (2023) Fast and accurate Estimation of evapotranspiration for smart agriculture. Water Resour Res 59(4). https://doi.org/10.1029/2023WR034535

Li W, Wainwright HM, Yan Q, Zhou H, Dafflon B, Wu Y, Versteeg R, Tartakovsky DM (2021) Estimation of evapotranspiration rates and root water uptake profiles from soil moisture sensor array data. Water Resour Res 57(11). https://doi.org/10.1029/2021WR030747

Maya Moreshwar Meshram S, Adla S, Jourdin L, Pande S (2024) Review of low-cost, off-grid, biodegradable in situ autonomous soil moisture sensing systems: is there a perfect solution? Comput Electron Agric 225:109289. https://doi.org/10.1016/j.compag.2024.109289

Mualem Y (1976) A new model for predicting the hydraulic conductivity of unsaturated porous media. Water Resour Res 12(3):513–522. https://doi.org/10.1029/WR012i003p00513

Nguyen MN, Hao Y, Baik J, Choi M (2021) Partitioning evapotranspiration based on the total ecosystem conductance fractions of soil, interception, and canopy in different biomes. J Hydrol 603:126970. https://doi.org/10.1016/j.jhydrol.2021.126970

Oleson KW, Niu G-Y, Yang Z, -L., Lawrence DM, Thornton PE, Lawrence PJ, Stöckli R, Dickinson RE, Bonan GB, Levis S, Dai A, Qian T (2008) Improvements to the community land model and their impact on the hydrological cycle. J Geophys Research: Biogeosciences 113(G1). https://doi.org/10.1029/2007JG000563

Orouskhani E, Sahoo S, Agyeman B, Bo S, Liu J (2023) Impact of sensor placement in soil water estimation: a real-case study. Irrig Sci 41:395–411. https://doi.org/10.1007/s00271-023-00845-y

Pauwels VRN, Verhoest NEC, De Lannoy GJM, Guissard V, Lucau C, Defourny P (2007) Optimization of a coupled hydrology–crop growth model through the assimilation of observed soil moisture and leaf area index values using an ensemble Kalman filter. Water Resour Res 43(4). https://doi.org/10.1029/2006WR004942

Pollacco JAP, Mohanty BP (2012) Uncertainties of water fluxes in soil–Vegetation–Atmosphere transfer models: inverting surface soil moisture and evapotranspiration retrieved from remote sensing. Vadose Zone J 11(3). https://doi.org/10.2136/vzj2011.0167

Reichle RH, Walker JP, Koster RD, Houser PR (2002) J Hydrometeorol 3(6):728–740. https://doi.org/10.1175/1525-7541(2002)003%3C0728:EVEKFF%3E2.0.CO;2. Extended versus Ensemble Kalman Filtering for Land Data Assimilation

Reichle RH, Crow WT, Koster RD, Sharif HO, Mahanama SPP (2008) Contribution of soil moisture retrievals to land data assimilation products. Geophys Res Lett 35(1). https://doi.org/10.1029/2007GL031986

Rezaei M, Seuntjens P, Joris I, Boënne W, Van Hoey S, Campling P, Cornelis WM (2016) Sensitivity of water stress in a two-layered sandy grassland soil to variations in groundwater depth and soil hydraulic parameters. Hydrol Earth Syst Sci 20(1):487–503. https://doi.org/10.5194/hess-20-487-2016

Schelle H, Durner W, Iden SC, Fank J (2013) Simultaneous Estimation of soil hydraulic and root distribution parameters from lysimeter data by inverse modeling. Procedia Environ Sci 19(0):564–573. https://doi.org/10.1016/j.proenv.2013.06.064

Schwärzel K, Menzer A, Clausnitzer F, Spank U, Häntzschel J, Grünwald T, Köstner B, Bernhofer C, Feger K-H (2009) Soil water content measurements deliver reliable estimates of water fluxes: a comparative study in a Beech and a Spruce stand in the Tharandt forest (Saxony, Germany). Agric for Meteorol 149(11):1994–2006. https://doi.org/10.1016/j.agrformet.2009.07.006

Shen X, Liang J, Zeleke KT, Liang Y, Wang G, Duan A, Mi Z, Ning H, Gao Y, Zhang J (2018) Optimizing the positioning of soil moisture monitoring sensors in winter wheat fields. Water 10(12):1707. https://doi.org/10.3390/w10121707

Šimůnek J, Hopmans JW (2009) Modeling compensated root water and nutrient uptake. Ecol Model 220(4):505–521. https://doi.org/10.1016/j.ecolmodel.2008.11.004

Sonkar I, Kotnoor HP, Sen S (2019) Estimation of root water uptake and soil hydraulic parameters from root zone soil moisture and deep percolation. Agric Water Manage 222. https://doi.org/10.1016/j.agwat.2019.05.037

Soulis KX, Elmaloglou S, Dercas N (2015) Investigating the effects of soil moisture sensors positioning and accuracy on soil moisture based drip irrigation scheduling systems. Agric Water Manage 148:258–268. https://doi.org/10.1016/j.agwat.2014.10.015

Strebel L, Bogena H, Vereecken H, Andreasen M, Aranda-Barranco S, Hendricks Franssen HJ (2024) Evapotranspiration prediction for European forest sites does not improve with assimilation of in situ soil water content data. Hydrol Earth Syst Sci 28(4):1001–1026. https://doi.org/10.5194/hess-28-1001-2024

van Genuchten MT (1980) A Closed-form equation for predicting the hydraulic conductivity of unsaturated soils. Soil Sci Soc Am J 44(5):892–898. https://doi.org/10.2136/sssaj1980.03615995004400050002x

Vereecken H, Huisman JA, Bogena H, Vanderborght J, Vrugt JA, Hopmans JW (2008) On the value of soil moisture measurements in vadose zone hydrology: A review. Water Resour Res 44(4). https://doi.org/10.1029/2008WR006829

Vitali V, Sutka M, Ojeda L, Aroca R, Amodeo G (2021) Root hydraulics adjustment is governed by a dominant cell-to-cell pathway in beta vulgaris seedlings exposed to salt stress. Plant Sci 306:110873. https://doi.org/10.1016/j.plantsci.2021.110873

Wang T, Xu Y, Zuo Q, Shi J, Wu X, Liu L, Sheng J, Jiang P, Ben-Gal A (2023) Evaluating and improving soil water and salinity stress response functions for root water uptake. Agric Water Manage 287:108451. https://doi.org/10.1016/j.agwat.2023.108451

Xiong M, Liu P, Cheng L, Deng C, Gui Z, Zhang X, Liu Y (2019) Identifying time-varying hydrological model parameters to improve simulation efficiency by the ensemble Kalman filter: a joint assimilation of streamflow and actual evapotranspiration. J Hydrol 568(November 2018):758–768. https://doi.org/10.1016/j.jhydrol.2018.11.038

Yu GR, Zhuang J, Nakayama K, Jin Y (2007) Root water uptake and profile soil water as affected by vertical root distribution. Plant Ecol 189(1):15–30. https://doi.org/10.1007/s11258-006-9163-y

Zhang X, Feng G, Sun X (2024) Advanced technologies of soil moisture monitoring in precision agriculture: a review. J Agric Food Res 18:101473. https://doi.org/10.1016/j.jafr.2024.101473